# On the design of discrete Voss nets and their generalizations

Georg Nawratil[1,2]

[1]Institute of Discrete Mathematics and Geometry, TU Wien
www.dmg.tuwien.ac.at/nawratil/

[2]Center for Geometry and Computational Design, TU Wien

# Co-Workers & Related Publications

## Part I

M. Kilian, G. N., M. Raffaelli, A. Rasoulzadeh, K. Sharifmoghaddam:
Interactive design of discrete Voss nets and simulation of their rigid foldings, Computer Aided Geometric Design (accepted, 2024)

## Part II

G. N.:
On continuous flexible Kokotsakis belts of the isogonal type & V-hedra with skew faces, Journal for Geometry and Graphics **26**(2):237–251 (2022)

# Part I

# Basics

A planar quad-surface (PQ-surface) is a plate-hinge structure made of quadrilateral panels connected by rotational joints in the combinatorics of a square grid.

A generic PQ-surface is rigid, but there exist certain classes allowing an isometric deformation having one degree of freedom.

One such class are **V-hedra**, which are discrete analogs of Voss (V) surfaces (i.e. smooth surfaces with a conjugate geodesic net) and date back to

Sauer, R., Graf, H.: Über Flächenverbiegung in Analogie zur Verknickung offener Facettenflache, Mathematische Annalen **105**:499–535 (1931)

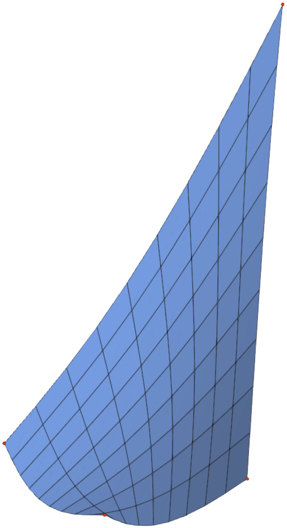

# Basics

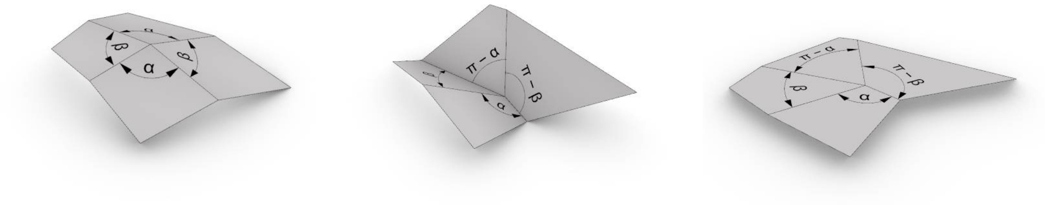


The geodesic condition translates into the equality of opposite angles at every vertex.

**Remark:** Discrete analogs of conjugate nets are PQ-surfaces, which dates back to

Peterson, K.: Ueber Curven und Flächen, A. Lang's Buchhandlung, Moskau; Franz Wagner, Leipzig (1868)

By replacing this equality condition by the closely related constraint that opposite angles at every vertex are supplementary, we get so-called **anti-V-hedra**.

# Basics

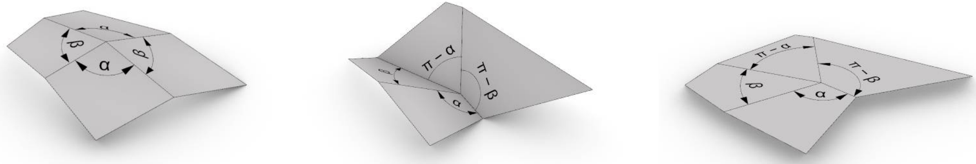


**V-hedra:** flat-foldable (flat self-overlapping position) in two different ways

**anti-V-hedra:** developable and flat-foldable

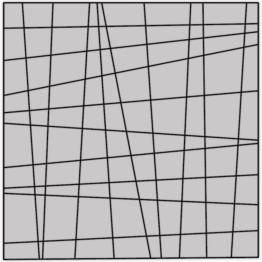

**Remark:** Every PQ-surface that is developable ($\alpha + \beta + \gamma + \delta = 2\pi$) and flat-foldable ($\alpha - \beta + \gamma + -\delta = 0$; Kawasaki's theorem) has to be an anti-V-hedron. Beside the degenerated case of developable V-hedra.

# Examples

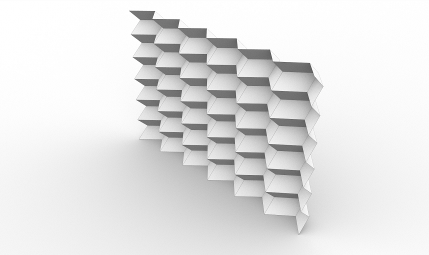

*Eggbox pattern* (V-hedron)

V-hedra have many applications in structural and mechanical engineering.

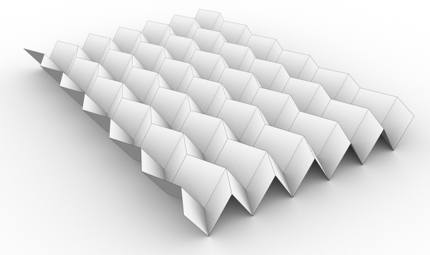

*Miura-ori* (anti-V-hedron)

Anti-V-hedra are of practical interest as they are developable and flat-foldable at the same time.

# Review

PQ-surfaces are rigid-foldable if and only if every $3 \times 3$ block has this property, cf.

Schief, W.K., Bobenko, A.I., Hoffmann, T.: On the integrability of infinitesimal and finite deformations of polyhedral surfaces, in: Discrete Differential Geometry, Springer, pp. 67–93 (2008)

First results on rigid-foldable $3 \times 3$ blocks were given by

Kokotsakis, A.: Über bewegliche Polyeder, Mathematische Annalen **107**:627–647 (1933)

containing the already known V-hedral case, but he also mentioned for the first time anti-V-hedral and hybrid $3 \times 3$ patches.

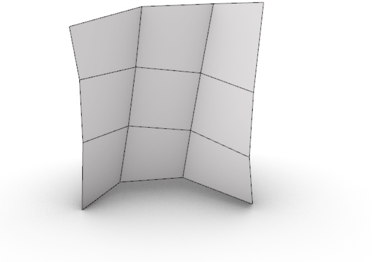

**Remark:** First examples of larger hybrid patches showing the transition from generalized Miura-ori to eggbox were given by

Tachi, T.: Freeform rigid-foldable structure using bidirectionally flat-foldable planar quadrilateral mesh, Advances in Architectural Geometry, Springer, pp. 87–102 (2010)

# Relation between V-vertex and anti-V-vertex

By extension of two adjacent faces to the other side a V-vertex can be transformed into an anti-V-vertex (and vice versa).

**Spherical image:** one of the four points of the spherical isogram (opposite sides have the same length) is replaced by its antipode.

$\Longrightarrow$ both cases can be unified using spherical kinematics, where it is known as the *isogonal* case (cf. Part II) according to

Stachel, H.: A kinematic approach to Kokotsakis meshes, Computer Aided Geometric Design **27**:428–437 (2010)

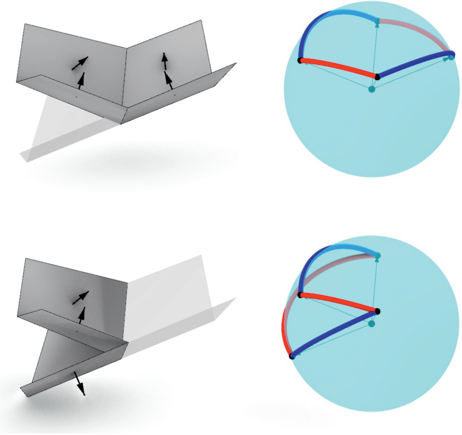

# Relation between V-vertex and anti-V-vertex

**Gauss map:** In a V-vertex opposite dihedral angles are equal due to reasons of symmetry $\Longrightarrow$ Gauss map is a spherical Chebyshev quad. In more detail it is a spherical parallelogram according to Eq. (5.12) of

Schief, W.K., Bobenko, A.I., Hoffmann, T.: On the integrability of infinitesimal and finite deformations of polyhedral surfaces, in: Discrete Differential Geometry, Springer, pp. 67–93 (2008)

By construction of an anti-V-vertex two adjacent normals flip in orientation $\Longrightarrow$ Gauss map is a spherical anti-parallelogram.

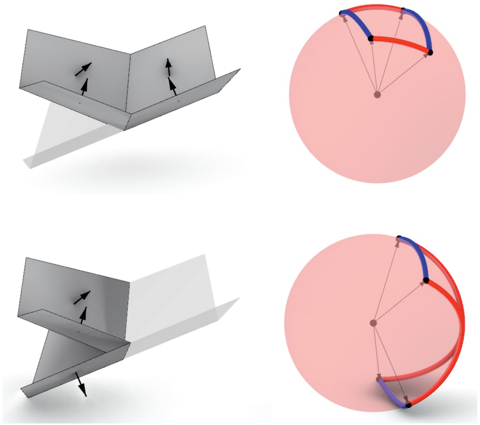

# Completing the Gauss map

*Assume that three pairwise distinct points* $\mathbf{b}, \mathbf{c}, \mathbf{d}$ *on the unit-sphere* $S^2$ *are given in a way that the plane* $\varepsilon$ *spanned by them does not contain the sphere center* $O$*. Compute a fourth point* $\mathbf{a} \in S^2$ *with:*

$$\|\mathbf{c}-\mathbf{d}\| = \|\mathbf{a}-\mathbf{b}\| \quad \text{and} \quad \|\mathbf{c}-\mathbf{b}\| = \|\mathbf{a}-\mathbf{d}\|.$$

Completing the spherical Chebyshev quad
by $\mathbf{a}^+$ to a spherical parallelogram
by $\mathbf{a}^-$ to a spherical anti-parallelogram

$\mathbf{a}^-$ is obtained by reflecting $\mathbf{c}$ on the bisecting plane of $\mathbf{b}$ and $\mathbf{d}$.
We obtain $\mathbf{a}^+$ by reflecting $\mathbf{a}^-$ on the plane $O, \mathbf{b}, \mathbf{d}$.

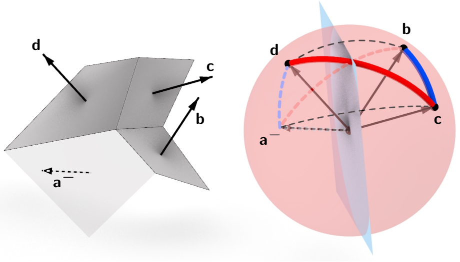

# Completing the Gauss map

*Assume that three pairwise distinct points* $\mathbf{b}, \mathbf{c}, \mathbf{d}$ *on the unit-sphere* $S^2$ *are given in a way that the plane* $\varepsilon$ *spanned by them does not contain the sphere center* $O$. *Compute a fourth point* $\mathbf{a} \in S^2$ *with:*

$$\|\mathbf{c} - \mathbf{d}\| = \|\mathbf{a} - \mathbf{b}\| \quad \text{and} \quad \|\mathbf{c} - \mathbf{b}\| = \|\mathbf{a} - \mathbf{d}\|.$$

Completing the spherical Chebyshev quad
by $\mathbf{a}^+$ to a spherical parallelogram
by $\mathbf{a}^-$ to a spherical anti-parallelogram

Alternatively $\mathbf{a}^+$ can be computed by a half-turn of $\mathbf{c}$ about the line spanned by $O$ and the midpoint of $\mathbf{b}$ and $\mathbf{d}$.

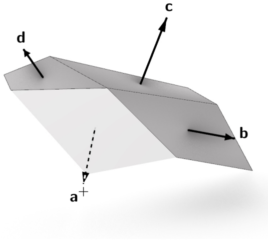


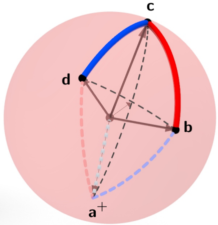

# Review on existing design methods/tools

**1)** Sauer sketched two methods for determining a V-hedron via control polylines in
Sauer, R.: Differenzengeometrie, Springer (1970)

**(a)** by two boundary polylines plus the direction of fold-lines

**(b)** by a zigzag diagonal

**2)** Anti-V-hedra were studied by
Feng, F., et al.: The designs and deformations of rigidly and flat-foldable quadrilateral mesh origami, Journal of the Mechanics and Physics of Solids **142**:104018 (2020)
Their marching algorithm to obtain the crease pattern is identical to Sauer's design method (a) applied to the anti-Voss condition.

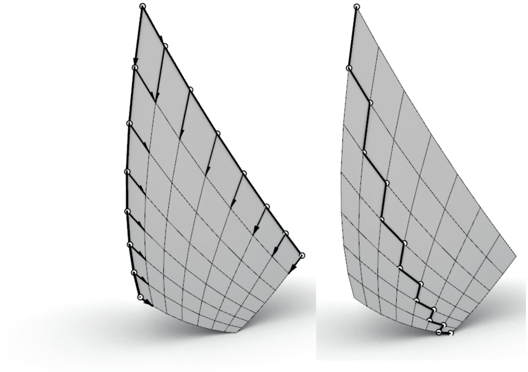

# Review on existing design methods/tools

**3)** Two design methods for V-hedra are discussed in

Montagne, N., et al.: Discrete Voss surfaces: Designing geodesic gridshells with planar cladding panels, Automation in Construction **140**:104200 (2022)

**(i)** exactly method (a) of Sauer, although the correct attribution is missing

**(ii)** Designing a discrete Chebyshev net on the sphere and then exploring the space of parallel V-hedra having the chosen Chebyshev net as Gauss map

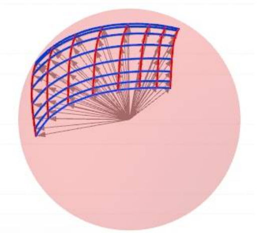

**4)** A design algorithm for anti-V-hedra was presented by

Lang, R.J., Howell, L.: Rigidly Foldable Quadrilateral Meshes From Angle Arrays, Journal of Mechanisms and Robotics **10**:021004 (2018) Software: FLATFORM

Modified version of Sauer's method (a) applied to anti-V-hedra in the developed state, where to each edge a folding angle is assigned.

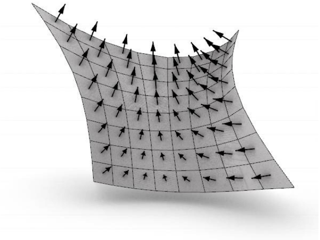

# Review on existing design methods/tools

**5)** A design tool for generating V-hedra, anti-V-hedra and hybrid surfaces is given by

Tachi, T.: Freeform rigid-foldable structure using bidirectionally flat-foldable planar quadrilateral mesh, Advances in Architectural Geometry, Springer, pp. 87–102 (2010) Software: FREEFORM ORIGAMI

The interactive tool allows drag motions of vertices, which deforms the perturbed net to its orthogonal projection on the set of bidirectionally flat-foldable planar quad-meshes.

**6)** Algorithm for the inverse design problem was presented in

Dang, X., et al.: Inverse design of deployable origami structures that approximate a general surface, International Journal of Solids and Structures 234-235:111224 (2022)

Approximation of a target surface by an anti-V-hedron with the mountain-valley assignment of Miura-ori.

# On the convexity of quads

According to the investigations of Kokotsakis given in

Kokotsakis, A.: Über bewegliche Polyeder, Mathematische Annalen **107**:627–647 (1933)

a necessary condition that a net with V-vertices and/or anti-V-vertices consists only of convex quads is that each $3 \times 3$ block has one of the following vertex assignments:

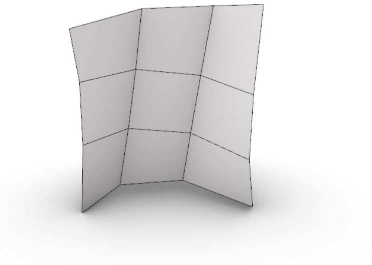

- all 4 vertices are either of V-type or anti-V-type
- 2 vertices are of V-type, 2 of anti-V-type

**Remark:** If this condition is violated at least one concave quad has to exist.

Studies dealing with anti-V-hedra a restricted to convex quads. V-hedra are discussed in

Sauer, R., Graf, H.: Über Flächenverbiegung in Analogie zur Verknickung offener Facettenflache, Mathematische Annalen **105**:499–535 (1931)

under the assumption of not flipped quads, but concave non-flipped quads are allowed.

# On the convexity of quads

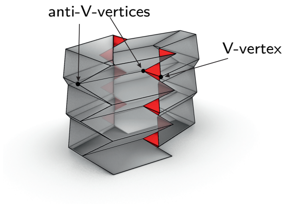


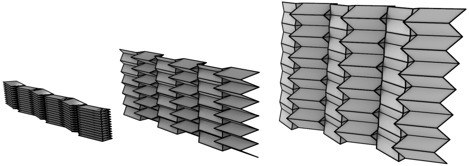

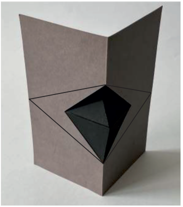

Known examples of flexible discrete surfaces containing concave quads:

1. Flipped quads are contained in the Miura-Tachi tubes

   Miura, K., Tachi, T.: Synthesis of rigid-foldable cylindrical polyhedra, Symmetry: Art and Science 2010, pp. 204–213 (2010)

2. Flipped quads are contained in a wall design (Croydon Colonnade)
3. Concave faces can be seen in the crinkle construction done by Connelly

   Connelly, R.: Flexing surfaces, The Mathematical Gardner, pp. 79–89 (1981)

# On the convexity of quads

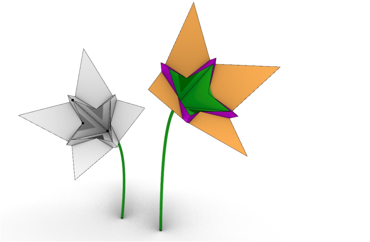

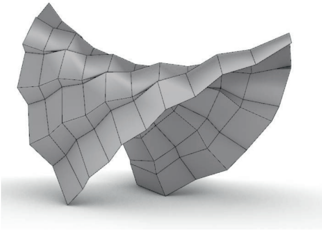

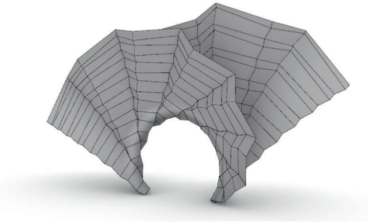

There is no need for this convexity restriction as it limits the design space artificially. For the same reason we allow flipped quads, which additionally enables us to discretize some surface singularities* without introducing vertices with a valence different than four.

**Open problem:** Which type of surface singularities can be modeled with this approach?

**Remark:** The flipped quads can also easily be built for practical application in an architectural scale; e.g. by welding two crossing beams.

*Conjugate lines of same family intersect.

# Flexibility of 3x3 blocks (without any restriction on quads)

A $3 \times 3$ block is continuous flexible if and only if the spherical image has this property; cf.

Stachel, H.: A kinematic approach to Kokotsakis meshes, Computer Aided Geometric Design **27**:428–437 (2010)

One can always find a proper orientation of the edges (pode, antipode) such that the spherical mechanism is only composed of spherical isograms; cf.

N. G.: On continuous flexible Kokotsakis belts of the isogonal type & V-hedra with skew faces, Journal for Geometry and Graphics **26**:237–251 (2022)

From the formulas given in these two publications one can see that any such linkage is continuous flexible if a non-flat initial position is given (cf. Part II).

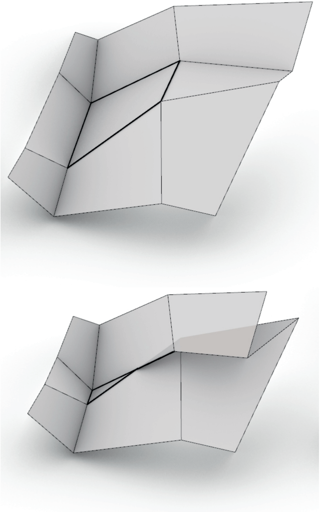

# Constructive algorithm (generalization of Sauer's methods)

We allow both types of vertices and generate the quad mesh in a non-flat state, therefore rigid-foldability is for free.

We developed a corresponding toolkit as part of the SCUTES add-on for Grasshopper/Rhino, which is an interactive plugin for the creation, manipulation and visualization of rigid-foldable quad surfaces.

Sharifmoghaddam, K., N. G., Rasoulzadeh, A., Tervooren, J.: Using flexible trapezoidal quad-surfaces for transformable design, Proc. of the IASS Annual Symposium 2020/21, pp. 3236–3248 (2021)

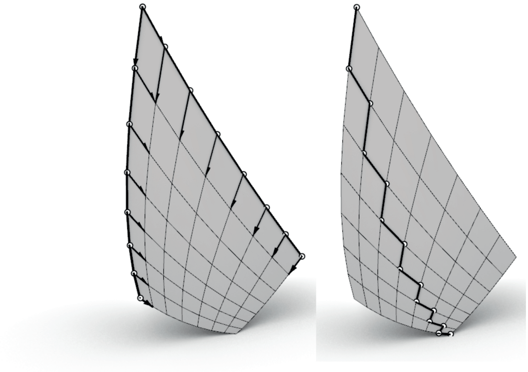

Present only diagonal zigzag method!

# Diagonal ZigZag: Workflow

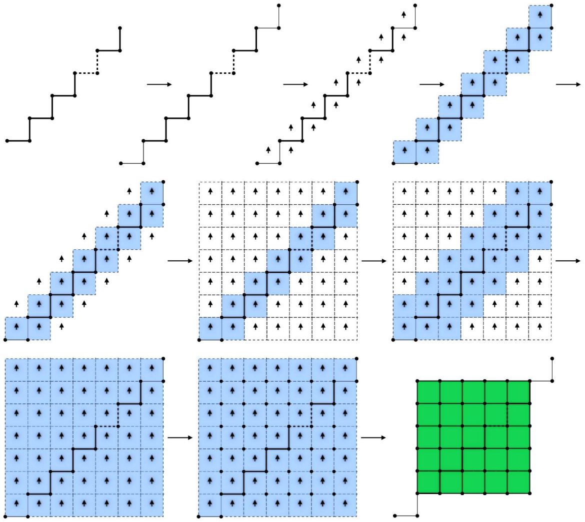

The normals around a vertex $\mathbf{x}$ are denoted by $\mathbf{a}, \mathbf{b}, \mathbf{c}, \mathbf{d}$. The signed distance of the corresponding faces to the origin is given by

$$a := \langle \mathbf{x}, \mathbf{a} \rangle \qquad b := \langle \mathbf{x}, \mathbf{b} \rangle$$
$$c := \langle \mathbf{x}, \mathbf{c} \rangle \qquad d := \langle \mathbf{x}, \mathbf{d} \rangle$$

Then $\mathbf{x}$ is a V-vertex or anti-V-vertex if and only if the following discrete Moutard equation holds:

$$\det \begin{pmatrix} a & b & c & d \\ \mathbf{a} & \mathbf{b} & \mathbf{c} & \mathbf{d} \end{pmatrix} = 0$$

Izmestiev, I., Raffaelli, M., Rasoulzadeh, A.: Voss surfaces (in preparation)

# Diagonal ZigZag: Final step

Once the data on the Gauss map and support function is available on the entire grid, one can compute the vertices via the following closed-form expression:

$$\mathbf{x} = \frac{1}{\det(\mathbf{c}-\mathbf{d}, \mathbf{c}-\mathbf{b}, \mathbf{c})} \begin{pmatrix} \mathbf{c}\times\mathbf{b} & \mathbf{d}\times\mathbf{c} & (\mathbf{c}-\mathbf{d})\times(\mathbf{c}-\mathbf{b}) \end{pmatrix} \begin{pmatrix} c-d \\ c-b \\ c \end{pmatrix}$$

Izmestiev, I., Raffaelli, M., Rasoulzadeh, A.: Voss surfaces (in preparation)

At this step the geometry of the involved quads is revealed, and flipped quads could happen naturally.
But the flipping of quads also affects the Voss and anti-Voss assignment of the vertices $\Longrightarrow$ post-processing

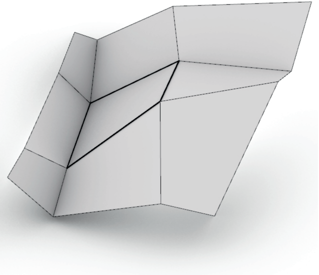

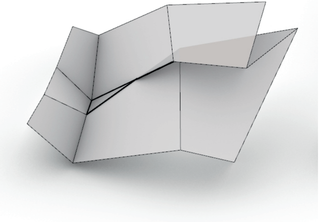

# Post-processing

Update the local face normals in each vertex to get a consistent data set of the mesh enabling the orientability of the surface, which is needed for generating mesh textures, signed distance fields for (self-)collision detection, ...

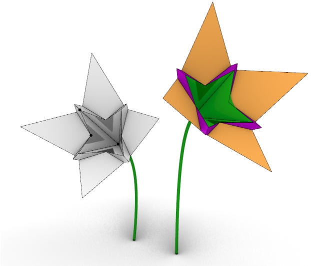

Examples revealed the existence of further vertex types beside Voss and anti-Voss in the generated meshes.

The systematic classification of vertices is based on a

**Generalized Definition of a vertex to be V-hedral and anti-V-hedral:**

A vertex $\mathbf{x}$ is called V-hedral if $\alpha^*$ equals $\alpha$ or $2\pi - \alpha$ and $\beta^*$ equals $\beta$ or $2\pi - \beta$ for $\alpha, \beta \in (0; \pi) \cap (\pi; 2\pi)$.
A vertex $\mathbf{x}$ is called anti-V-hedral if $\alpha^*$ equals $|\pi - \alpha|$ and $\beta^*$ equals $|\pi - \beta|$ for $\alpha, \beta \in (0; \pi) \cap (\pi; 2\pi)$.

# Post-processing: Motivation for Redefinition

Definition covers following cases:

**(i)** The construction principle of reversing one edge can also be applied to the case $\alpha > \pi$.

**(ii)** One faces of an ordinary V-vertex is replaced by its complement to the full circle.

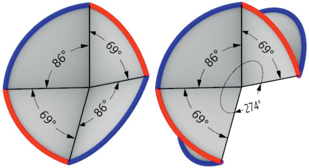


Chebyshev quad

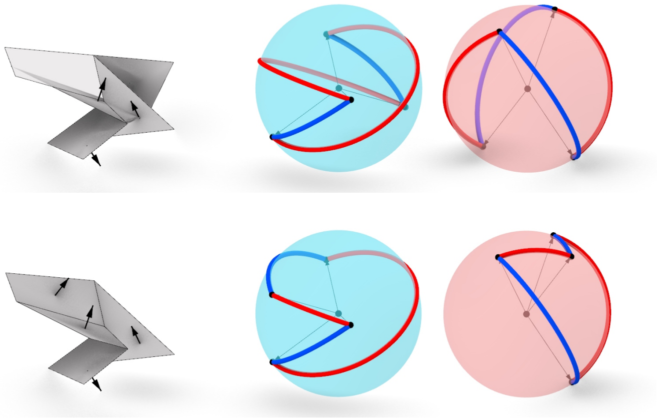

anti-Chebyshev quad

# Post-processing: Systematic classification of V-vertices

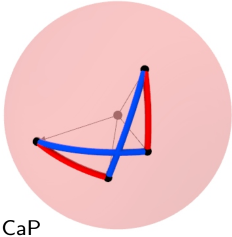

CaP

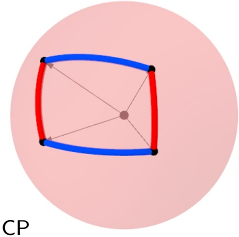

CP

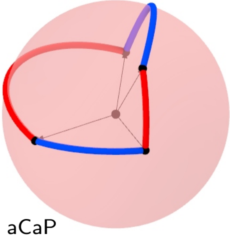

aCaP

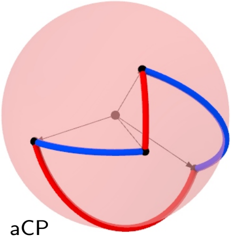

aCP

Impossible to realize without self-intersection

VCaP

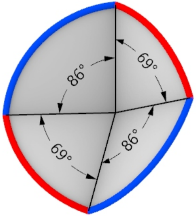


VCP

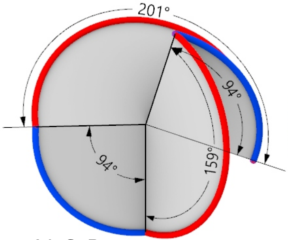


VaCaP

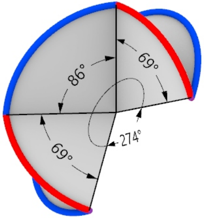


VaCP

# Post-processing: Systematic classification of anti-V-vertices

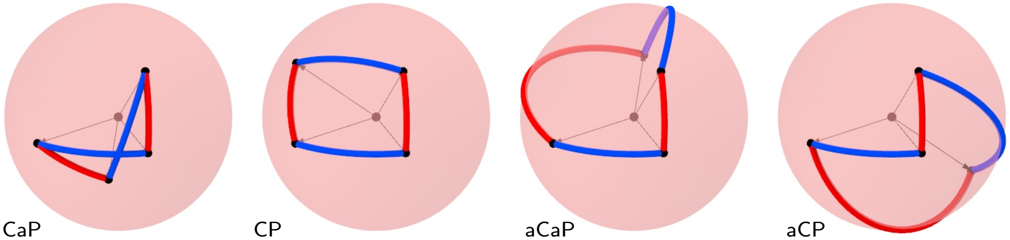


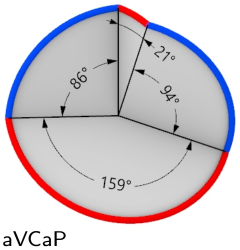


aVCP

Impossible to
realize without
self-intersection

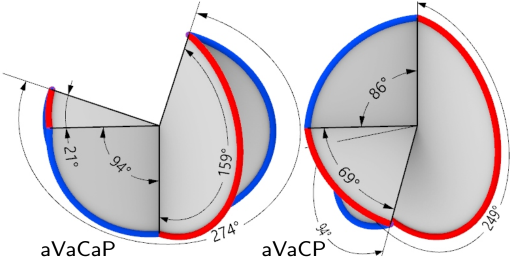

# Diagonal ZigZag: Rigid-folding

We decrease computational complexity by deforming the input (diagonal zigzag) and regenerating the mesh, instead of applying transformations to the generated mesh as e.g. done in

Feng, F., et al.: The designs and deformations of rigidly and flat-foldable quadrilateral mesh origami, Journal of the Mechanics and Physics of Solids **142**:104018 (2020)

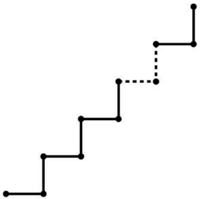

**A)** Check the vertex types along the diagonal of the generated mesh (post-processing).
**B)** Deform the diagonal according to the transformation formulas for the dihedral angles:

$$\text{V-vertex:} \quad \tan\left(\pm\tfrac{\mu}{2}\right) \to t\tan\left(\pm\tfrac{\mu}{2}\right) \qquad \tan\left(\pm\tfrac{\nu}{2}\right) \to \tfrac{1}{t}\tan\left(\pm\tfrac{\nu}{2}\right)$$

$$\text{anti-V-vertex:} \quad \tan\left(\pm\tfrac{\mu}{2}\right) \to t\tan\left(\pm\tfrac{\mu}{2}\right) \qquad \tan\left(\pm\tfrac{\nu}{2}\right) \to t\tan\left(\pm\tfrac{\nu}{2}\right)$$

**Remark:** Forward kinematics of a serial robot with rotational joints, where consecutive rotation axes intersect. Moreover, the rotation angles are known functions in $t$.

# Diagonal ZigZag: Examples

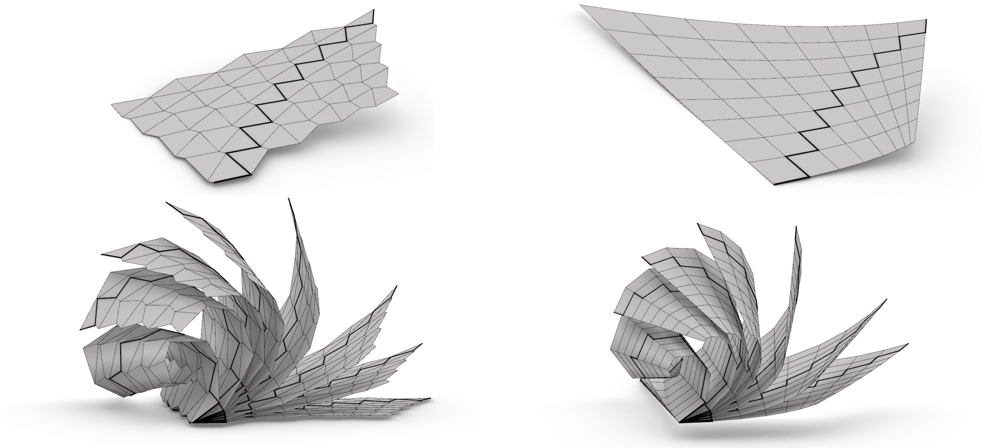

**Open problem:** How to assign the two possible normals to the faces in such a way that the resulting surface has no self-intersections and is close to some desired geometry?

# Approximation Algorithm

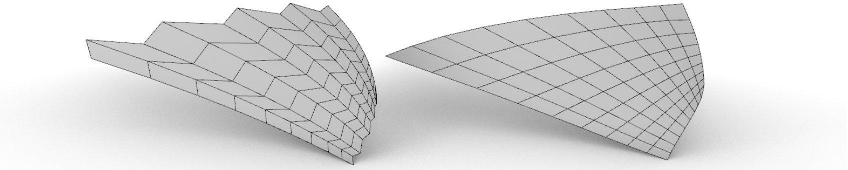

Given an input quad mesh and we optimize for face planarity, fairness, and (anti-)Voss property; while the corners are fixed. The implemented iterative algorithm is based on

Tang, C., et al.: Form-finding with polyhedral meshes made simple, ACM Trans. Graphics **33**(4):70 (2014)

(anti-)Voss conditions: $\langle \mathbf{a}, \mathbf{b} \rangle - \langle \mathbf{c}, \mathbf{d} \rangle = 0 \quad \langle \mathbf{a}, \mathbf{d} \rangle - \langle \mathbf{c}, \mathbf{b} \rangle = 0$

# Approximation Algorithm

The algorithm can be adjusted to allow the user to constrain the position of any vertex.

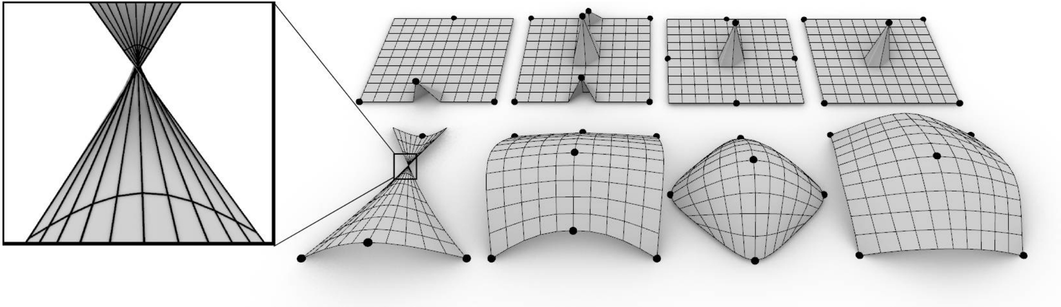

A crucial assumption is the smoothness of the output mesh. The formulation of our fairness term does not support the generation of anti-V-hedra or hybrid versions.

**Open problem:** How to adapt the fairness term?

# Approximation Algorithm: Folding Simulation

The algorithm does not result in an exact Voss net $\Longrightarrow$ Simulation of the folding motion

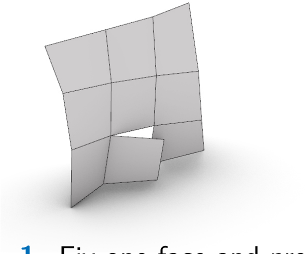

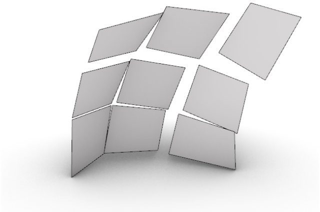

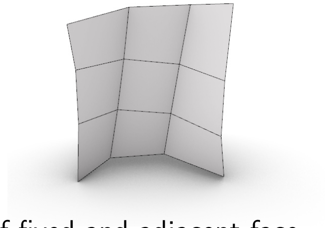

1. Fix one face and prescribe the angle between normals of fixed and adjacent face.
2. Break the complete mesh up to a quad soup.
3. Minimize the distance between corresponding vertices in the quad soup.

**Remark:** Alternative minimization functions can be used; e.g. distance between corresponding line-segments or the closely related elastic joint energy.

# Comparing Example

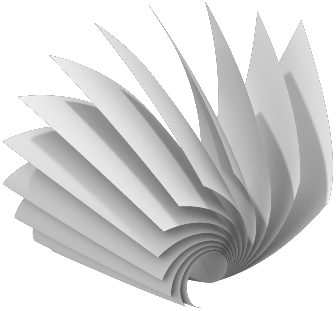

Smooth Voss surface patch $\Upsilon$ and its isometric deformation.

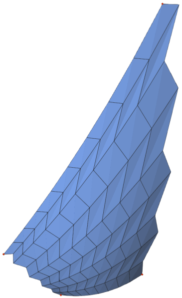

Discretization plus random noise. Input of the Approximation Algorithm.

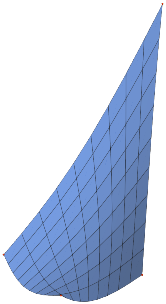

Output $V_1$ of the Approximation Algorithm.

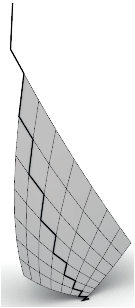

V-hedron $V_2$ by extracting one of $V_1$'s diagonals.

# Comparing Example

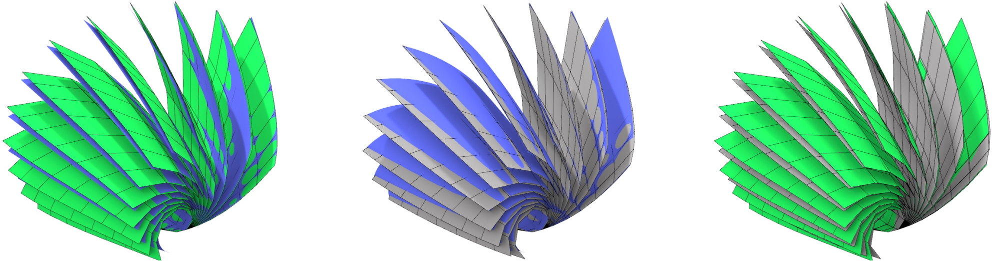

For the computation we folded the first dihedral angle for both approaches in 44 steps of 1 degree change, but only every fourth step is illustrated above with $\Upsilon$ (blue), $V_1$ (green) and $V_2$ (gray).

# Part II

# Kokotsakis* studied the following problem in 1932

**Given is a rigid closed polygonal line p (planar or non-planar), which is surrounded by a polyhedral strip, where at each polygon vertex three faces meet. Determine the geometries of these closed strips with a continuous mobility.**

In general these loop structures are rigid, thus continuous flexible ones possess a so-called overconstrained mobility.
Kokotsakis himself only studied flexible belts with planar polygons p.

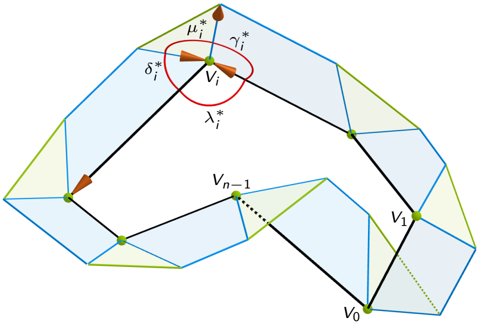


---

* Kokotsakis, A.: Über bewegliche Polyeder, Mathematische Annalen **107**:627–647 (1932)

# Review

Kokotsakis only obtained general results (arbitrary $n$) for the isogonal type; i.e. in every vertex both pairs of opposite angles are (1) equal or (2) supplementary;

$$(1)\quad \lambda_i^* = \mu_i^*, \qquad \delta_i^* = \gamma_i^*,$$
$$(2)\quad \lambda_i^* + \mu_i^* = \pi, \qquad \delta_i^* + \gamma_i^* = \pi.$$

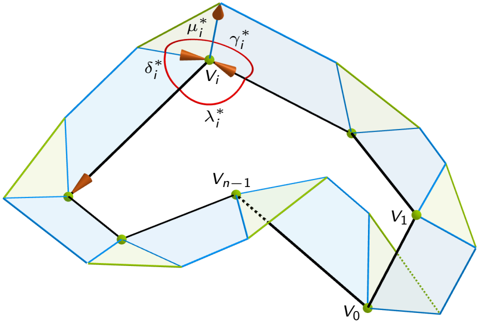


## Special cases

**n=3:** Bricard octahedra of the 3rd type.

**n=4:** $3 \times 3$ building blocks of V-hedra, anti-V-hedra and the hybrid case.

# Goal

**We generalize Kokotsakis' problem by allowing the faces, which are adjacent to polygon line-segments, to be skew. We do not restrict to planar polygons p but to the isogonal type.**

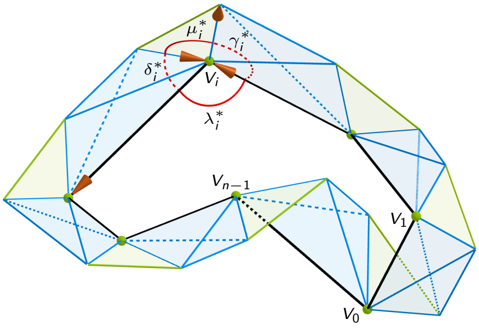

# Spherical image of the original Kokotsakis belts

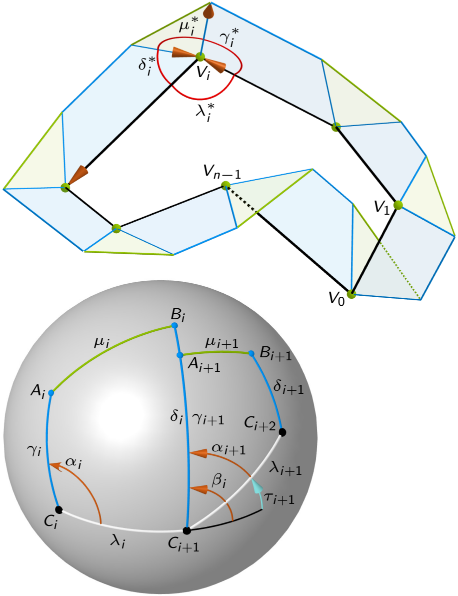


A Kokotsakis belt is continuous flexible if and only if its spherical image has this property; cf.
Stachel, H.: A kinematic approach to Kokotsakis meshes, Computer Aided Geometric Design **27**:428–437 (2010)

Taking the orientation of the line-segments into account, the spherical 4-bar mechanism, which corresponds with the arrangement of faces around the vertex $V_i$, has spherical bar lengths:

$$\delta_i = \pi - \delta_i^*, \qquad \gamma_i = \pi - \gamma_i^*,$$
$$\lambda_i = \pi - \lambda_i^*, \qquad \mu_i = \pi - \mu_i^*.$$

# Spherical image of the original Kokotsakis belts

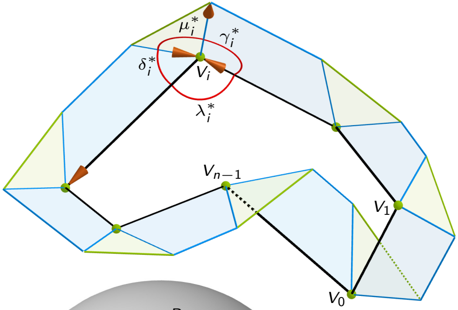


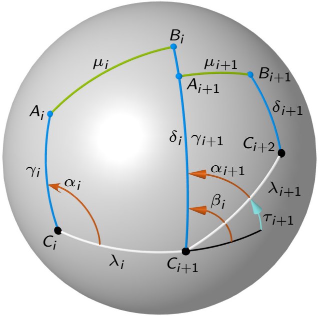


The spherical image of faces around two adjacent vertices $V_i$ and $V_{i+1}$ corresponds to two coupled spherical 4-bar mechanisms.

The dihedral angles $\beta_i$ and $\alpha_{i+1}$ are related by the torsion angle $\tau_{i+1}$ of the polygon p.

**Remark:** Note that p is a planar curve if all $\tau_{i+1}$ are either zero or $\pi$.

# Spherical image of the generalized Kokotsakis belts

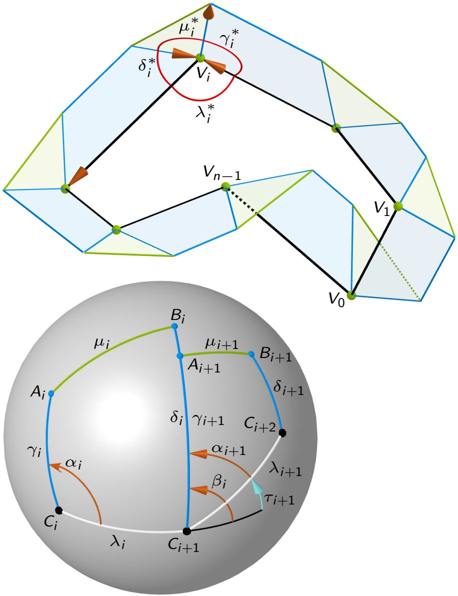


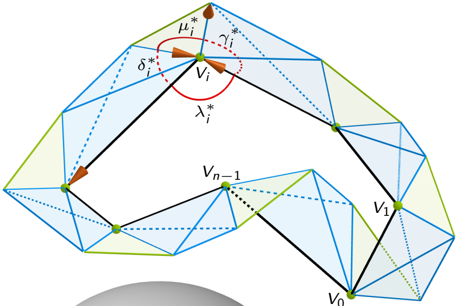


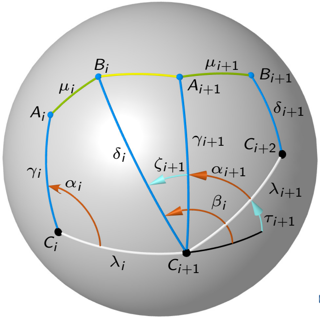


The non-planarity of the faces imply that $B_i, C_{i+1}, A_{i+1}$ are not longer on a great circle.

# Spherical isogram

In the isogonal case these 4-bar mechanisms are

$$\begin{aligned} &(1)\ \lambda_i = \mu_i, && \delta_i = \gamma_i, \\ &(2)\ \lambda_i + \mu_i = \pi, && \delta_i + \gamma_i = \pi. \end{aligned}$$

Type (2) is obtained from the spherical isogram (1) by the replacement of one of the vertices by its antipodal point. Without loss of generality we can restrict to type (1) by assuming an appropriate choice of orientations.

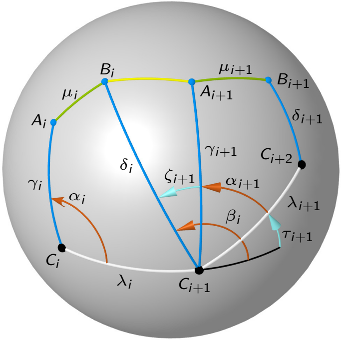

# Spherical kinematics

The input angle $\alpha_i$ and the output angle $\beta_i$ of the $i$-th spherical isogram are related by

$$b_i = f_i a_i \quad \text{with} \quad f_i = \frac{\sin\delta_i \pm \sin\lambda_i}{\sin(\delta_i - \lambda_i)} \neq 0 \qquad (\star)$$

where $a_i = \tan\frac{\alpha_i}{2}$ and $b_i = \tan\frac{\beta_i}{2}$; cf.
Stachel, H.: A kinematic approach to Kokotsakis meshes, Computer Aided Geometric Design **27**:428–437 (2010)

The shift between the output angle $\beta_i$ of the $i$-th isogram to the input angle $\alpha_{i+1}$ of the $(i+1)$-th isogram is given by the offset angle $\varepsilon_{i+1}$ consisting of the twist angle $\zeta_{i+1}$ and the torsion angle $\tau_{i+1}$; i.e.

$$a_{i+1} = \frac{b_i + e_{i+1}}{1 - b_i e_{i+1}} \quad \text{with} \quad e_{i+1} = \tan\frac{\varepsilon_{i+1}}{2}. \qquad (\bullet)$$

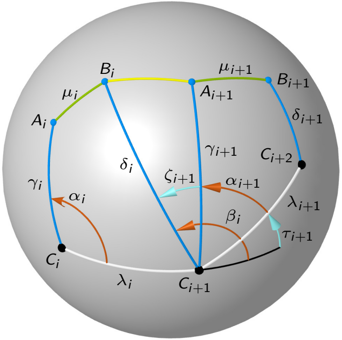

# Solving the stated problem

Firstly, we formulate the so-called *closure condition*

$$a_0 - a_n = 0.$$

Within this condition we substitute $a_n$ by

$$a_n = \frac{a_{n-1} f_{n-1} + e_n}{1 - a_{n-1} f_{n-1} e_n}$$

which results from (●) under consideration of (⋆).
By iterating this kind of substitution we end up with

$$q_2 a_0^2 + q_1 a_0 + q_0 = 0,$$

where $q_i$s are functions in $f_0, \ldots, f_{n-1}, e_0, \ldots, e_{n-1}$.

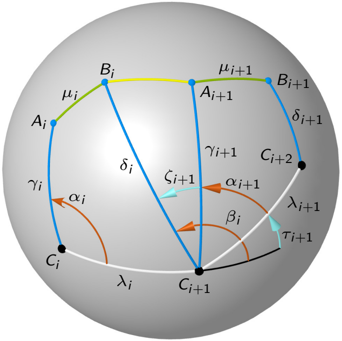

# Solving the stated problem

Thus the necessary and sufficient conditions for continuous mobility are:

$$q_0 = 0, \quad q_1 = 0, \quad q_2 = 0.$$

**Theorem 1.**

For a given closed polygon p with $n$ vertices, there exists at least a $(2n-3)$-dimensional set of continuous flexible Kokotsakis belts of the isogonal type over $\mathbb{C}$.

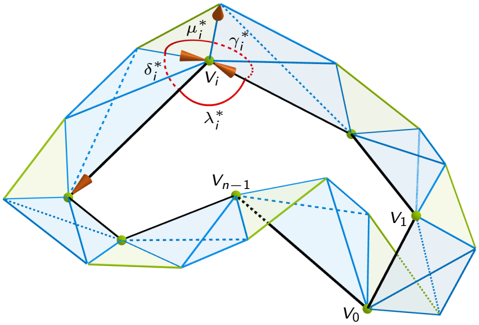

# Solving the stated problem

Thus the necessary and sufficient conditions for continuous mobility are:

$$q_0 = 0, \quad q_1 = 0, \quad q_2 = 0.$$

**Theorem 2.**

For a given closed polygon p with $n > 3$ vertices, there exists at least a $(n-3)$-dimensional set of continuous flexible Kokotsakis belts with planar faces of the isogonal type over $\mathbb{C}$. For planar polygons p this dimension raises to $(n-1)$; as only the condition $f_0 f_1 \dots f_{n-1} = 1$ remains*.

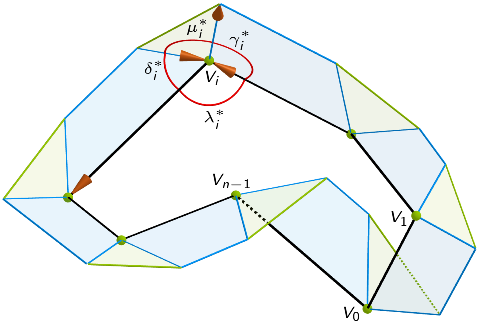


* This implies continuous flexibility for a non-flat initial configuration (cf. Part I).

# Property regarding the rotation angles

Dihedral angles along opposite edges meeting in a vertex $V_i$ have at each time instant the same absolute value of their angular velocities.

Thus the absolute values of the rotation angles around these two edges are the same (measured from an initial configuration).

The same absolute values of the rotation angle can always be assigned to three edges.

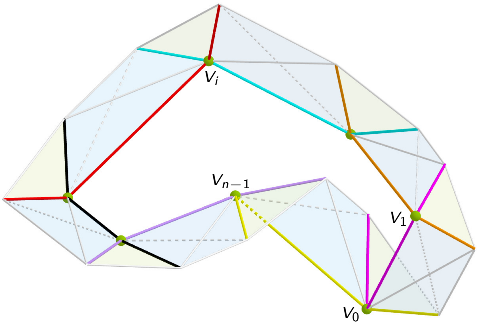

# Example: n=3

For any choice of $\delta_i$ and $\lambda_i$ with $\lambda_1 + \lambda_2 + \lambda_3 = 2\pi$ there exist $e_0, e_1, e_2 \in \mathbb{C}$ such that we get a continuous flexible Kokotsakis belt of the isogonal type.

The resulting structure can be seen as an overconstrained 6R loop, which belongs to the third class of so-called angle-symmetric 6R linkages given in

Li, Z., Schicho, J.: Classification of angle-symmetric 6R linkages, Mech. Mach. Theory **70**:372–379 (2013)

**Remark:** Note that for $e_0 = e_1 = e_2 = 0$ we get a Bricard octahedron of the 3rd type.

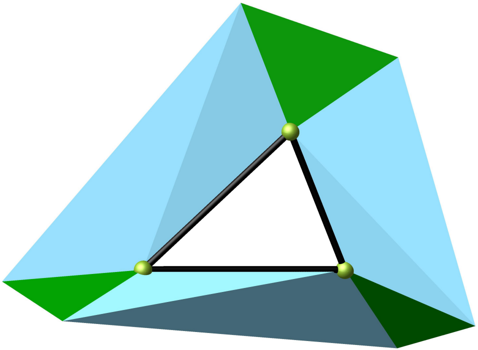

# Continuous flexible skew-quad (SQ) surfaces

Vorgegeben sei ein Vierecksnetz mit starren und i.a. nicht-ebenen Vierecksmaschen. Bei der Realisierung etwa durch ein Blechmodell kann man die Vierecke durch irgend welche Flächenstücke, z.B. durch Ausschnitte aus hyperbolischen Paraboloiden, ausfüllen. Wir nehmen an, daß das Vierecksnetz mindestens drei Leitstreifen einer jeden der beiden Scharen, also 3 × 3 Vierecksmaschen, enthält. Ein solches Vierecksnetz ist i.a. s t a r r, d.h. es läßt keine Verknickungen durch Drehung benachbarter Maschen um die jeweils gemeinsame Maschenseite zu, ohne daß es zu einer Zerreißung des Netzes kommt. Wir haben aber auch Vierecksnetze kennen gelernt, die eine 1-parametrige Menge von Verknickungen zulassen (v e r k n i c k b a r e V i e r e c k s n e t z e), nämlich die V-Netze in § 12 und die T-Netze in § 13. Dabei handelte es sich um ebenflächige Vierecksnetze; ob es auch nicht-ebenflächige verknickbare Vierecksnetze gibt, ist ein ungelöstes Problem. Bei den Verknickungen

The following open problem:

**Do there exist rigid-foldable SQ surfaces?**

is mentioned on page 168 of Sauer's book

Sauer, R.: Differenzengeometrie, Springer (1970)

A key result for answering this question is the following generalization of a theorem by

Schief, W.K., Bobenko, A.I., Hoffmann, T.: On the integrability of infinitesimal and finite deformations of polyhedral surfaces, in: Discrete Differential Geometry, Springer, pp. 67–93 (2008)

**Theorem 3.**

A non-degenerate SQ surface is continuous flexible, if and only if this holds true for every $3 \times 3$ building block.

# Building block of a V-hedron with skew quads

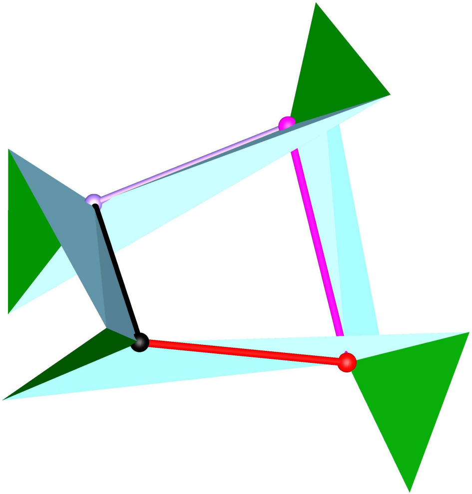

A $3 \times 3$ building block of a V-hedron with skew quads (left) and its spherical image (right).

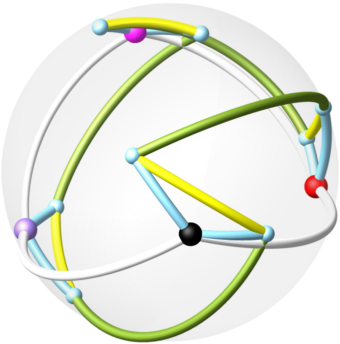

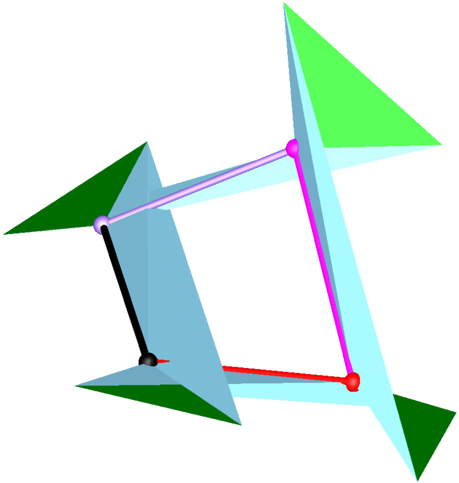

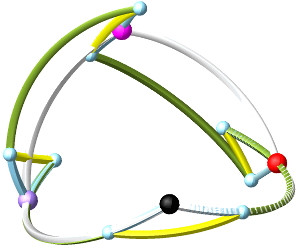

# Lower bound on the dimension of the design space

This bound $q$ can be obtained by comparing the number $q_{par}$ of free parameters for constructing a $([3+t]\times[3+s])$ skew quad mesh with the number $q_{con}$ of algebraic conditions needed to make the mesh isogonal and continuous flexible.

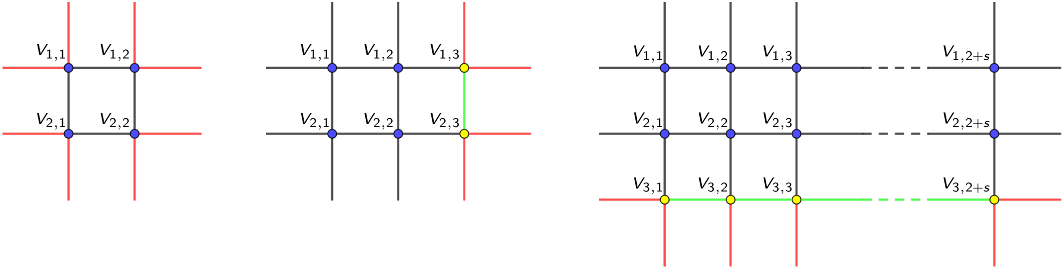


$$q_{par} = 21 + 10s + 10t + 3st,$$
$$q_{con} = 11 + 7s + 7t + 5st.$$

# Lower bound on the dimension of the design space

Thus finally we get the lower bound $q$ by:

$$q := q_{par} - q_{con} - 1 = 9 + 3s + 3t - 2st.$$

The subtraction of 1 comes from the fact that the structure has a 1-dimensional mobility.

| t\s | 0 | 1 | 2 | 3 | 4 | 5 | 6 | 7 | 8 | 9 | 10 | 11 | 12 | 13 | 14 | 15 | $i > 15$ |
|---|---|---|---|---|---|---|---|---|---|---|---|---|---|---|---|---|---|
| 0 | 9 | 12 | 15 | 18 | 21 | 24 | 27 | 30 | 33 | 36 | 39 | 42 | 45 | 48 | 51 | 54 | 9+3i |
| 1 | | 13 | 14 | 15 | 16 | 17 | 18 | 19 | 20 | 21 | 22 | 23 | 24 | 25 | 26 | 27 | 12+i |
| 2 | | | 13 | 12 | 11 | 10 | 9 | 8 | 7 | 6 | 5 | 4 | 3 | 2 | 1 | 0 | $<0$ |
| 3 | | | | 9 | 6 | 3 | 0 | $<0$ | $<0$ | $<0$ | $<0$ | $<0$ | $<0$ | $<0$ | $<0$ | $<0$ | $<0$ |
| 4 | | | | | 1 | $<0$ | $<0$ | $<0$ | $<0$ | $<0$ | $<0$ | $<0$ | $<0$ | $<0$ | $<0$ | $<0$ | $<0$ |
| 5 | | | | | | $<0$ | $<0$ | $<0$ | $<0$ | $<0$ | $<0$ | $<0$ | $<0$ | $<0$ | $<0$ | $<0$ | $<0$ |
| $\vdots$ | | | | | | | $\ddots$ | $\ddots$ | $\ddots$ | $\ddots$ | $\ddots$ | $\ddots$ | $\ddots$ | $\ddots$ | $\ddots$ | $\ddots$ | $\vdots$ |

It remains open if a continuous flexible SQ surface of infinite dimension in rows and columns exists. **Maybe the answer is already hidden in ...**

# Related recent Work & Open problems

Motivated by V-hedra with skew quads a research group at KAUST also studied flexible $3 \times 3$ arrangements of skew quads and obtained a classification for these meshes in

Liu, Y., Ouyang, Y., Michels, D.L.: On the Algebraic Classification of Non-singular Flexible Kokotsakis Polyhedra, arXiv:2401.14291 (2024)

An interesting subclass is discussed in more detail in

Aikyn, A., et al.: Flexible Kokotsakis Meshes with Skew Faces: Generalization of the Orthodiagonal Involutive Type, Computer-Aided Design **168** (2024)

which corresponds to skew analogs of so-called T-hedra, which are the topic of tomorrow's talk given by

**Kiumars Sharifmoggadam:** *"Exploring T-hedral Origami across varied Topologies"*

**Open problem:** What are the smooth analogs of continuous flexible Kokotsakis belts of the isogonal type and of V-hedra with skew quads?

# Associated overconstrained mechanism

**Definition: Reciprocal-parallel quad meshes $\mathcal{Q}$ and $\mathcal{V}$**

- ⋆ $\mathcal{Q}$ and $\mathcal{V}$ are combinatorial dual; i.e. vertices correspond to faces and vice versa.
- ⋆ The edges of adjacent faces are mapped to edges between corresponding adjacent vertices and vice versa. Moreover, corresponding edges are parallel.

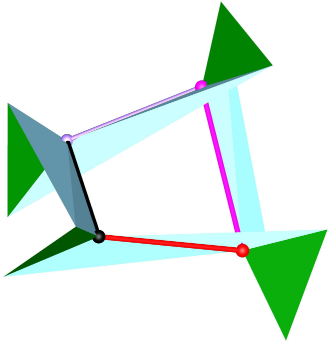

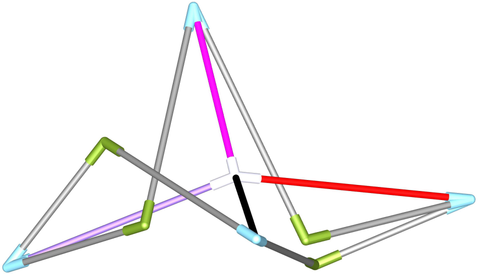

# Associated overconstrained mechanism

Every infinitesimal flexible quad surface $\mathcal{Q}$ possesses in general a unique (up to scaling) reciprocal-parallel quad mesh $\mathcal{V}$; cf.

Sauer, R.: Differenzengeometrie, Springer (1970)

The corresponding deformation of $\mathcal{V}$ during the continuous flexion of $\mathcal{Q}$ has to be a conformal transformation, as the vertex stars are rigid.

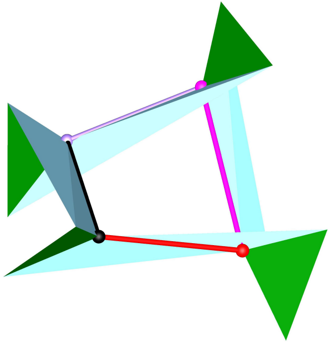

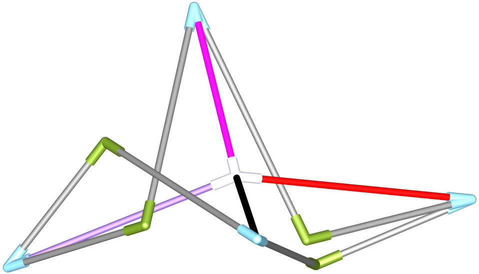

# Associated overconstrained mechanism

Sauer also showed that the vertex star fulfilling the isogonality condition is reciprocal-parallel to a skew isogram, which has the following additional property: If the four bars of the isogram are hinged in the vertices by rotational joints, which are orthogonal to the plane spanned by the linked bars, then one obtains a so-called *Bennett mechanism*.

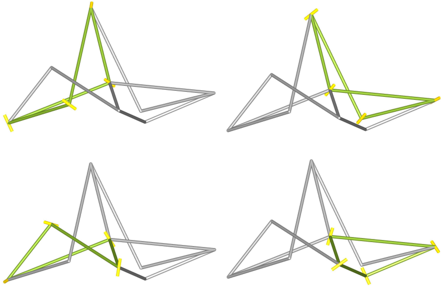

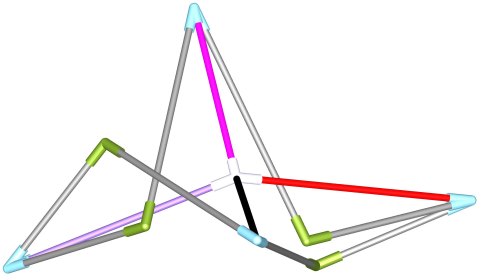

# Associated overconstrained mechanism

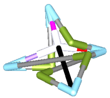

The corresponding overconstrained mechanism consists of rigid vertex stars linked by cylindrical joints and one rotational joint.

**Acknowledgment**

The research is supported by project F77 (SFB "Advanced Computational Design") of the Austrian Science Fund.

advanced computational design

# Thanks